VOLUME 115, NUMBER 13
JUNE 30, 1993

JOURNAL
OF THE
AMERICAN
CHEMICAL
SOCIETY

Local Raman Tensors of Double-Helical DNA in the Crystal: A Basis for Determining DNA Residue Orientations†

James M. Benevides,‡ Masamichi Tsuboi,‡,§ Andrew H.-J. Wang,∥ and George J. Thomas, Jr.*,‡

Contribution from the Division of Cell Biology and Biophysics, School of Biological Sciences, University of Missouri—Kansas City, Kansas City, Missouri 64110, and Biophysics Division and Department of Cell and Structural Biology, University of Illinois, Urbana-Champaign, Urbana, Illinois 61801

Received December 3, 1992

Abstract: We report the first experimental determination of Raman scattering tensors for localized base and sugar–phosphate vibrations of double-helical DNA. Argon-laser excitation was employed in combination with a multichannel Raman microscope system to measure polarized Raman scattering intensities from oriented single crystals of d(CGCGCG) in the left-handed Z conformation. The Raman measurements were made on crystals of dimensions $abc = 30 \times 50 \times 70$ μm in space group $P2_12_12_1$, for which the three-dimensional structure has been solved by X-ray methods.[1,2] For each intense band in the 300–1700-cm^{-1} interval of the Raman spectrum, we determined the relative scattering intensities, I_{aa}, I_{bb}, and I_{cc}, corresponding to the *aa*, *bb*, and *cc* components of the crystal Raman tensors. The tensor quotients from the crystal were augmented with measured depolarization ratios of analogous Raman bands in the solution isotropic form of Z-DNA and its nucleotide constituents. From these data, we have calculated the shapes and orientations of localized, vibration-specific, Raman scattering tensors applicable to normal modes of the bases (625 (dG), 670 (dG), 784 (dC), 1264 (dC), 1318 (dG), 1486 (dG), and 1579 (dG) cm^{-1}), phosphate–ester moieties (749, 796, 868, and 1095 cm^{-1}), and furanose substituents (1426 and 1433 cm^{-1}). The results differentiate normal modes with polarizability changes in the planes of the bases (dC or dG), from those perpendicular to the base planes, and along specific bond-angle bisectors (OPO, HCH). These findings provide a basis for future applications of Raman microscopy as a probe of DNA orientation and anisotropy in biological complexes.

Introduction

Raman spectroscopy is a convenient and versatile probe of nucleic acid structure. The method is suited to small and large nucleic acids and their complexes in aqueous solutions (H_2O and D_2O) and in crystalline and noncrystalline solids. The applicability of Raman spectroscopy over wide ranges of solution temperature and composition facilitates its use in the study of many biologically important structure transitions. A review of principles, methods, and current applications has been given.[3] Recent advances in instrumentation have also contributed to an expanding role for Raman spectroscopy as a structural probe of highly condensed states of chromosomal DNA in eukaryotic cells and viruses.[4–6]

Empirical approaches have been developed by several groups

† Supported by NIH Grant AI18758.
‡ University of Missouri.
§ Permanent Address: Department of Fundamental Sciences, Iwaki-Meisei University, Iwaki, Fukushima 970, Japan.
∥ University of Illinois.
* Author to whom correspondence may be addressed.

(1) Wang, A. H.-J.; Fujii, S.; van Boom, J. H.; van der Marel, G. A.; van Boeckel, S. A.; Rich, A. *Nature* **1982**, *299*, 601–604.
(2) Gessner, R. V.; Frederick, C. A.; Quigley, G. J.; Rich, A.; Wang, A. H.-J. *J. Biol. Chem.* **1989**, *264*, 7921–7935.
(3) Thomas, G. J., Jr.; Tsuboi, M. *Adv. Biophys. Chem.* **1993**, *3*, 1–69.
(4) Puppels, G. J.; de Mul, F. F. M.; Otto, C.; Greve, J.; Robert-Nicoud, M.; Arndt-Jovin, D. J.; Jovin. T. M. *Nature* **1990**, *347*, 301–303.

0002-7863/93/1515-5351$04.00/0

of investigators to correlate Raman bands of mononucleotides, oligonucleotides, and nucleic acids with distinctive structural features.[7-11] Ultimately, the extraction of structural information about DNA or RNA from the Raman spectrum requires: (i) reliable assignment of the spectral bands to specific vibrational modes of nucleotide residues, and (ii) knowledge of the dependence of band position and intensity upon the detailed three-dimensional structures of nucleic acid segments. In order to advance the latter, Raman signatures have been cataloged for oligonucleotide single crystals of known structure, as established by X-ray crystallography.[11-14] Although the crystal X-ray/Raman correlations developed for A, B, and Z forms of DNA are highly useful,[15] full advantage of the Raman spectrum remains to be realized. On the one hand, current Raman band assignments are far from complete. Of the more than 40 prominent bands in the spectrum of DNA, less than 10 have been well characterized by means of empirical correlations. Second, the intrinsic relationship between spectral intensity and molecular orientation is, surprisingly, not known for a single Raman band of DNA.

Each Raman band of DNA corresponds to a molecular vibration, which is usually localized within a well-defined group of atoms of a base or sugar–phosphate residue, and during which there occurs a change in amplitude of the dipole moment induced by the incident radiation. For each such localized vibration, there is associated a *Raman tensor*, the elements of which express directional changes of polarizability during vibration. For the n^{th} vibrational mode, each Raman tensor component, α_{ij}^n (where $i, j = x, y, z$ and $\alpha_{ij}^n = \alpha_{ji}^n$), is defined as a first derivative of the polarizability with respect to the vibrational normal coordinate. The Raman tensor components for the given normal mode define an ellipsoid in the molecular frame of reference. The principal axes (x, y, and z) of the ellipsoid are related in a simple manner to the orientation of the local vibrating group(s) of atoms in question. By imposing polarized incident radiation on uniformly oriented molecules (such as those in the unit cell of a single crystal of known structure), and by quantitative analysis of the polarization characteristics of the Raman scattered radiation, it is possible to determine the relative magnitudes of the Raman tensor components and relate these to local orientations of the vibrating molecular subgroups. In this work, we describe for the first time a determination of the orientations of the principal axes of the Raman tensors for double-helical DNA of known three-dimensional structure.

This investigation is facilitated by recent developments in instrumentation for Raman microscopy[4,6,16] and extends ongoing interest in the Raman depolarization properties of nucleotide model compounds.[17] Our analysis encompasses all major Raman bands of left-handed Z-DNA in the spectral region 300–1700 cm^{-1}. The target structure, d(CGCGCG), is known to high resolution by X-ray crystallography,[1] and its Raman signature has been well established in previous investigations.[12,18] The d(CGCGCG) crystal structure is favored for this study because of the location of the base planes nearly parallel to the crystallographic *ab* plane and nearly perpendicular to the crystallographic *c*-axis. Therefore, the out-of-plane and in-plane Raman tensor components for base-residue vibrations are expected to correspond, respectively, to *cc* and either *aa* or *bb* Raman tensor components of the crystal. The present study thus provides new information about the location of Raman tensors for conformation-sensitive vibrations of the DNA backbone. We discuss the significance of these results as a basis for future exploitation of polarized Raman microscopy to probe DNA base and backbone orientations in complex biological assemblies.

Materials and Methods

1. Samples for Raman Spectroscopy. The oligonucleotide, d(CGCGCG), was synthesized by an improved phosphate triester method in which 1-hydroxybenzotriazole was used as an activating agent.[19] After being deblocked, the fragment was purified by Sephadex-G50 column chromatography and converted to the ammonium salt. The purity of the oligomer was greater than 95% as judged by HPLC analysis. Crystallization of the d(CGCGCG) duplex followed procedures described for the X-ray structure determination.[20] The d(CGCGCG) crystal exhibits an elongated hexagonal cross section as shown in Figure 1.

Crystals of d(CGCGCG) were transferred with approximately 20 μL of mother liquor [2-methyl-2,4-pentanediol (20%), 30 mM sodium cacodylate (pH 6.0), and 30 mM $MgCl_2$] to a microsampling cell which was thermostated at 11 °C. The cell was constructed from an octagonally shaped (25-mm diagonal) glass slide onto which was mounted a cylindrical collar (3-mm height × 13-mm diameter) to contain crystals and mother liquor and a thin cover glass cap, as shown in Figure 2.

Poly(dG–dC)·poly(dG–dC) (Pharmacia, Lot No. AH7910106) was dissolved to 50 mg/mL in 4.0 M NaCl solution. Aliquots of 10 μL were sealed in glass capillaries (Kimax #34507), from which spectra were recorded as described previously.[21]

2. Instrumentation and Methods of Data Measurement. (a) Raman Microscopy of d(CGCGCG) Single Crystals. Raman spectra of single crystals of d(CGCGCG) were excited with both 514.5- and 488.0-nm excitation from an argon laser (Coherent, Innova 70–2). The radiant power at the laser head was maintained below 250 mW, which corresponds to less than 25 mW at the sample. The spectra were collected on a computer-controlled, triple-monochromator Raman microscope system (ISA/Jobin-Yvon Model S3000), employing a thermoelectrically cooled, 1024-channel, intensified diode-array detector (Princeton Instruments, Model IRY1024G/R). Differences in detector sensitivity for different channels were corrected by calibration with white light transmitted through the monochromator system to the detector. Reported Raman frequencies are accurate to ±1 cm^{-1}.

The sample-illuminating confocal microscope (Olympus, Model BHSM), which represents the optical core of this system, is shown in Figure 2. It is fitted with an 80× objective of 15-mm focal length. For optimal alignment and focusing of the laser beam with respect to the sample, a camera (NEC NC-15 CCD) and color monitor (NEC PM-1271A) were connected to the objective. As shown in Figure 2, the incident laser beam is directed through the objective onto the sample and the Raman scattering at 180° is collected with the same objective. For present experiments, the electric vector of the exciting radiation was directed horizontally on the microscope stage, i.e. along the *X*-axis in Figure 2. A polarizer was placed in front of the entrance slit to the monochromator, allowing transmittance only of Raman-scattered light polarized along the *X*-axis. An important advantage of this sampling arrangement for examining single crystals of known (crystallographic) axis orientation is the ability to collect Raman scattering of different polarizations without directly rotating the incident electric vector. Instead, the crystal is rotated

(5) Aubrey, K. L.; Casjens, S. R.; Thomas, G. J., Jr. *Biochemistry* **1992**, *31*, 11835–11842.
(6) Kubasek, W. L.; Wang, Y.; Thomas, G. A.; Patapoff, T. W.; Schoenwaelder, K.-H.; Van der Sande, J. H.; Peticolas, W. L. *Biochemistry* **1986**, *25*, 7440–7445.
(7) Lord, R. C.; Thomas, G. J., Jr. *Spectrochim. Acta* **1967**, *23A*, 2551–2591.
(8) Erfurth, S. C.; Kiser, E. J.; Peticolas, W. L. *Proc. Natl. Acad. Sci. U.S.A.* **1972**, *69*, 938–941.
(9) Lafleur, L.; Rice, J.; Thomas, G. J., Jr. *Biopolymers* **1972**, *11*, 2423–2437.
(10) Nishimura, Y.; Tsuboi, M.; Sato, T.; Akoi, K. *J. Mol. Struct.* **1986**, *146*, 123–153.
(11) Thomas, G. J., Jr.; Benevides, J. M.; Prescott, B. *Biomol. Stereodyn.* **1986**, *4*, 227–254.
(12) Benevides, J. M.; Wang, A. H.-J.; van der Marel, G. A.; van Boom, J. H.; Rich, A.; Thomas, G. J., Jr. *Nucleic Acids Res.* **1984**, *12*, 5913–5925.
(13) Benevides, J. M.; Wang, A. H.-J.; Rich, A.; Kyogoku, Y.; van der Marel, G. A.; van Boom, J. H.; Thomas, G. J., Jr. *Biochemistry* **1986**, *25*, 41–50.
(14) Benevides, J. M.; Wang, A. H.-J.; van der Marel, G. A.; van Boom, J. H.; Thomas, G. J., Jr. *Biochemistry* **1988**, *27*, 931–938.
(15) Thomas, G. J., Jr.; Wang, A. H.-J. *Nucleic Acids Mol. Biol.* **1988**, *2*, 1–30.
(16) Tsuboi, M.; Ikeda, T.; Ueda, T. *J. Raman Spectrosc.* **1991**, *22*, 619–626.
(17) Ueda, T.; Ushizawa, K.; Tsuboi, M. *Biopolymers*, in press.
(18) Thamann, T.; Lord, R. C.; Wang, A. H.-J.; Rich, A. *Nucleic Acids Res.* **1981**, *9*, 5443–5457.
(19) van der Marel, G. A.; van Boeckel, C. A. A.; Willie, G.; van Boom, J. H. *Tetrahedron Lett.* **1981**, 3887.
(20) Wang, A. H. J.; Quigley, G. J.; Kolpak, F. J.; Crawford, J. L.; Van Boom, J. H.; Van der Marel, G.; Rich, A. *Nature* **1979**, *282*, 680–686.

(a)

(b)

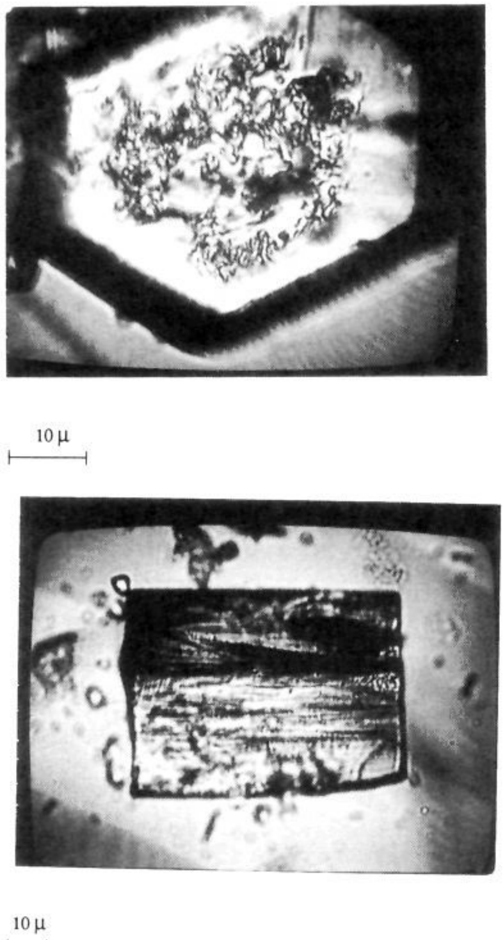

Figure 1. Photographs of single crystals of d(CGCGCG) employed for polarized Raman spectroscopy. (a) View along the crystallographic *c*-axis, perpendicular to the *ab* plane. (b) View along the crystallographic *a*-axis, perpendicular to the *bc* plane.

with respect to the incident light, thus minimizing possible polarization artifacts associated with the spectrograph analyzing polarizer and gratings. The angle of rotation of the crystal is controlled accurately by use of a precision microscope stage (Olympus BH2-SRG) in combination with the video camera and monitor assembly.

Spectra over the region 300–1700 cm^{-1}, displayed in the illustrations to follow, are the unsmoothed averages of 20–30 exposures obtained with an integration time of 60 s per exposure and spectral slit width of 7 cm^{-1}. Data collection and processing were performed with the ISA/Jobin-Yvon software operating on an IBM microcomputer. To enhance resolution in the 760–830-cm^{-1} interval, the signal-averaged data were fitted to a sum of Gauss–Lorentz curves by a nonlinear least-squares procedure (Spectra Calc Software, Galactic Industries). Prior to curve-fitting, the band envelope was smoothed with a 13-point convolution procedure.

(b) Depolarization Ratios of Z-DNA and Nucleotides. Polarized Raman spectra of the Z-DNA crystal structure were augmented by depolarization ratios measured on each corresponding band in isotropic Z-DNA. Spectra of poly(dG–dC)·poly(dG–dC) in 4.0 M NaCl solution were excited in the 90° scattering geometry using the 514.5-nm line of the argon laser. Data were collected on a scanning double-spectrometer system (Spex Ramalog V/VI) under the control of an IBM microcomputer.[21] Poly(dG–dC)·poly(dG–dC) exhibited a single sharp marker band at 625 cm^{-1}, diagnostic of the C3′-endo/syn deoxyguanosine conformer.[15] Depolarization ratios were obtained by placing a polarizer and scrambler in the path of the Raman-scattered radiation between the sample and monochromator entrance slit. The system was calibrated with liquid CCl_4, for which the 313- and 459-cm^{-1} bands exhibited apparent depolarization ratios ($\rho = I_\perp/I_\parallel$) of 0.744 and 0.006, corrected to 0.75 and 0.00, respectively. Table I lists depolarization ratios determined for bands of Z-DNA. Error limits of measured depolarization ratios are

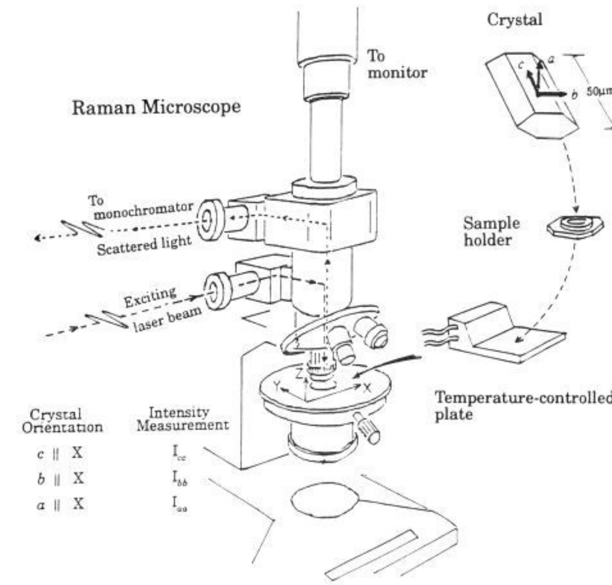

Figure 2. Diagram of the Raman microscope, illustrating the coordinate systems defined for polarization of the laser electric vector (X, Y, Z) and crystallographic unit cell (a, b, c). Also indicated are the intensities (I_{aa}, I_{bb}, I_{cc}) corresponding to specific orientations of the electric vector and crystallographic axes.

Table I. Depolarization Ratios of Selected Raman Bands of Z-DNA and Related Nucleotides[a]

		depolarization ratio (ρ)		
band (cm^{-1})	assignment	Z-DNA[b]	GMP[c]	CMP[c]
1581	guanine ring	0.33 ± 0.02	0.34	
1486	guanine ring	0.14 ± 0.01	0.113	
1427	CH_2 scissor[d]	0.4 ± 0.1	0.4	0.4
1318	guanine ring	0.31 ± 0.01	0.30	
1266	cytosine ring	0.29 ± 0.02		0.25
1095	PO_2^- stretch	0.06[e]		
868	backbone	<0.2		
785	cytosine ring	0.12 ± 0.01[f]		0.064
752	P–O stretch	<0.3		
626	guanine ring	0.07 ± 0.03	0.11	
596	cytosine ring	0.17 ± 0.05		0.16

[a] From solutions of randomly oriented molecules as described in the text. [b] Poly(dG–dC)·poly(dG–dC) at 50 mg/mL in 4.0 M NaCl solution. [c] Data from refs 3 and 17. [d] Values of 0.4 are also observed in other model compounds. See, for example: Sadtler Standard Spectra, Sadtler Research Laboratories, Philadelphia, 1973, Nos. 311R, 337R, and 630R. [e] Value transferred from the 1095-cm^{-1} band of dimethyl phosphate ion (Y. Guan and G. J. Thomas, Jr., unpublished results). For Z-DNA, the value of ρ (<0.1) is not accurately measurable to two significant figures. [f] Overlapped cytosine (784 cm^{-1}) and backbone (796 cm^{-1}) bands.

determined largely by the uncertainty in the intensity of the perpendicular component ($I_\perp$), as indicated in Table I, and in the references cited.

3. Theoretical Background and Procedure of Analysis. The d(CGCGCG) crystal has the space group $P2_12_12_1$ and unit cell dimensions a = 18.01 Å, b = 31.03 Å, and c = 44.80 Å. Its atomic coordinates are contained in File No. 304 of the Brookhaven Protein Data Bank.[2] The asymmetric unit contains one hexamer duplex, consisting of six deoxycytidines, six deoxyguanosines, and 10 phosphodiesters. We relate the principal axes (x, y, and z) of the Raman tensor localized at one of these residues to the crystallographic axes (a, b, and c) as follows. The tensor component of the crystal $\alpha_{FF'}$ is expressed in terms of the tensor component of the residue $\alpha_{gg'}$ by the relation:

$$\alpha_{FF'} = \sum \Phi_{Fg} \cdot \Phi_{F'g'} \cdot \alpha_{gg'} \quad (1)$$

where F and F' are a, b, or c; g and g' are x, y, or z; Φ is a direction cosine; and the sum is over g and g'. The direction cosines are defined explicitly as follows. Let l_x, m_x, n_x be direction cosines of the local x-axis placed in the rectangular abc-coordinate system; l_y, m_y, n_y are those for the y-axis, and l_z, m_z, n_z are those for the z-axis. For each hexamer duplex in the crystal, there are three duplex molecules related through the respective 2_1 operations around a, b, and c. The 2-fold rotations about a correspond to respective sign changes of m_x,m_y,m_z and n_x,n_y,n_z, leaving l_x,l_y,l_z unchanged. Likewise, the 2-fold rotations about b leave only the signs of m_x,m_y,m_z unchanged, and the 2-fold rotations about c leave only the signs of n_x,n_y,n_z unchanged. Therefore, if a normal vibration of the hexamer duplex occurs in-phase among the four duplexes of the unit cell (corresponding to a crystal mode of A_1 symmetry species of point group $D_2 \cong V$, which is isomorphous with space group $P2_12_12_1$), only α_{aa}, α_{bb}, and α_{cc} are non-zero:

$$\alpha_{aa} = 4(l_x^2\alpha_{xx} + l_y^2\alpha_{yy} + l_z^2\alpha_{zz}) \quad (2a)$$

$$\alpha_{bb} = 4(m_x^2\alpha_{xx} + m_y^2\alpha_{yy} + m_z^2\alpha_{zz}) \quad (2b)$$

$$\alpha_{cc} = 4(n_x^2\alpha_{xx} + n_y^2\alpha_{yy} + n_z^2\alpha_{zz}) \quad (2c)$$

$$\alpha_{ab} = \alpha_{bc} = \alpha_{ca} = 0 \quad (2d)$$

On the other hand, if two molecules related by the operation 2_1 along the a-axis execute normal vibrations with 180° phase difference, and simultaneously two molecules related by the operation 2_1 along b also vibrate with 180° phase difference (corresponding to symmetry species B_2 of group D_2), then $\alpha_{ab} \neq 0$. Similar relations hold for vibrations of symmetry species B_1 (α_{bc}) and B_3 (α_{ac}), for which the non-zero tensors are respectively

$$\alpha_{ab} = 4(l_xm_x\alpha_{xx} + l_ym_y\alpha_{yy} + l_zm_z\alpha_{zz}) \quad (3)$$

$$\alpha_{bc} = 4(m_xn_x\alpha_{xx} + m_yn_y\alpha_{yy} + m_zn_z\alpha_{zz}) \quad (4)$$

$$\alpha_{ac} = 4(l_xn_x\alpha_{xx} + l_yn_y\alpha_{yy} + l_zn_z\alpha_{zz}) \quad (5)$$

Thus, the crystalline Raman tensor components, α_{ab}, α_{bc}, and α_{ac}, of the $P2_12_12_1$ crystal of d(CGCGCG) are theoretically observable. However, our preliminary calculations, similar to those that follow, indicate that the tensor off-diagonal components (eqs 3–5) are much smaller than the diagonal components (eqs 2a–c), and the corresponding Raman bands are too weak to be observed. Therefore, no further consideration is given here to the components α_{ab}, α_{bc}, and α_{ac}.

Within the hexamer duplex, no residues are rigorously equivalent. For example, each of the six deoxycytidine residues has, in principle, a unique Raman spectrum with unique Raman tensors. However, these six sets of Raman bands cannot be resolved experimentally from one another, and in practice, the deoxycytidines may be regarded as "equivalent", i.e. a single set of Raman bands is observed, representing the average of all six dC residues. The same quasi-equivalency applies to the six deoxyguanosines, and also (to a good approximation) to the 10 phosphodiesters. (A notable exception occurs for the so-called "ring breathing mode" of guanine, which is significantly coupled to the sugar moiety and exhibits significant dependency of band frequency upon sugar pucker.[10,12] The distinctive contributions from C3'-endo/syn and C2'-endo/syn dG residues are easily resolved in our spectra and can be considered separately in the following analysis.) Therefore, eq 2 may be rewritten as:

$$\alpha_{aa} = 4[\sum(l_{xi})^2\alpha_{xx} + \sum(l_{yi})^2\alpha_{yy} + \sum(l_{zi})^2\alpha_{zz}] \quad (6)$$

where the sums over i represent the nearly equivalent groups in the hexamer duplex. Likewise, corresponding expressions may be written for α_{bb} and α_{cc}, following appropriate substitutions in eqs 3 and 4. Definition of the parameters, $r_1 = \alpha_{xx}/\alpha_{zz}$ and $r_2 = \alpha_{yy}/\alpha_{zz}$, allows expressions for the Raman intensity ratios of the crystal to be written as:

$$\frac{I_{aa}}{I_{bb}} = \frac{[\sum(l_{xi})^2r_1 + \sum(l_{yi})^2r_2 + \sum(l_{zi})^2]^2}{[\sum(m_{xi})^2r_1 + \sum(m_{yi})^2r_2 + \sum(m_{zi})^2]^2} \quad (7)$$

$$\frac{I_{bb}}{I_{cc}} = \frac{[\sum(m_{xi})^2r_1 + \sum(m_{yi})^2r_2 + \sum(m_{zi})^2]^2}{[\sum(n_{xi})^2r_1 + \sum(n_{yi})^2r_2 + \sum(n_{zi})^2]^2} \quad (8)$$

The data may be increased by measurement of the depolarization ratio, $\rho = I_\perp/I_\parallel$, for an isotropic distribution of molecular groups. For linearly polarized radiation, ρ is related to r_1 and r_2 by the expression:

$$\rho = \frac{1.5[(r_1 - r_2)^2 + (r_2 - 1)^2 + (1 - r_1)^2]}{5(r_1 + r_2 + 1)^2 + 2[(r_1 - r_2)^2 + (r_2 - 1)^2 + (1 - r_1)^2]} \quad (9)$$

To analyze each Raman tensor of the d(CGCGCG) crystal, we have adopted the following procedure:

(1) Arbitrarily select three nonlinearly arranged atoms, A, E1, and E2, of the local group. Choose the orientations of the three principal axes (x, y, and z) of the local Raman tensor by defining the y-axis parallel to the line connecting atoms E1 and E2, and the x-axis parallel to the line connecting atom A with the y-axis. The z-axis is defined perpendicular to the plane containing A, E1, and E2. The principal axes selected in this manner for several atomic groups of d(CGCGCG) are shown in Figure 3. The atoms selected as A, E1, and E2 for each set of principal axes are given in Table II.

(2) Calculate the nine direction cosines (l_x, ..., n_z) on the basis of the atomic coordinates of A, E1, and E2, as determined by the X-ray crystal structure.[2]

(3) Repeat the calculations for all nearly equivalent residues of the hexamer duplex, thus obtaining all members of the set l_{xi}, ..., n_{zi}, and by addition obtain $\sum(l_{xi})^2$, ..., $\sum(n_{zi})^2$.

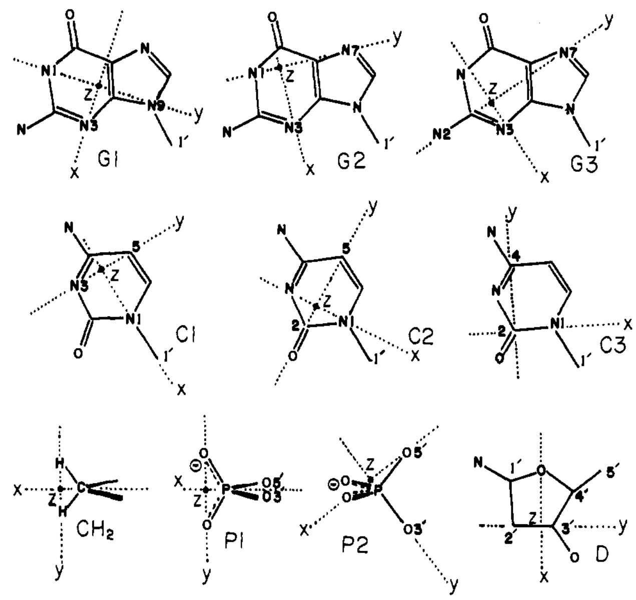

Figure 3. Principal axes (x, y, and z) of local Raman tensors representing selected base, sugar, and phosphate group vibrations of d(CGCGCG), as described in the text and Tables II–V. The coordinate systems are designated G1–G3 for guanine ring vibrations, C1–C3 for cytosine ring vibrations, CH_2 for methylene scissoring, P1 and P2 for phosphodioxy and phosphodiester stretching, and D for deoxyribose ring stretching. Within the limits of the present data, these coordinate systems (or alternatives involving permutations of x, y, and z) represent all reasonable choices for the Raman tensor calculations.

Table II. Principal Axes for Localizied Vibrational Modes of Z-DNA

system[a]	residue	atoms used to define axes: A	E1	E2
G1	guanine	N3	N1	N9
G2	guanine	N3	N1	N7
G3	guanine	N3	N2	N7
C1	cytosine	N1	N3	C5
C2	cytosine	N1	C2	C5
C3	cytosine	N1	C2	C4
CH_2	methylene	C	H	H[b]
P1	phosphate	P	O	O
P2	phosphate	O5′	P	O3′
D	deoxyribose	O4′	C2′	C3′

[a] See Figure 3. [b] Coordinates of the hydrogen atoms are not known. For $C5'H_2$, the axes (x,y,z) were defined with A = C5′, E1 = O5′, and E2 = C4′; then y and z were interchanged. For $C2'H_2$, x, y, and z were defined with A = C2′, E1 = C1′, and E2 = C3′; then y and z were interchanged.

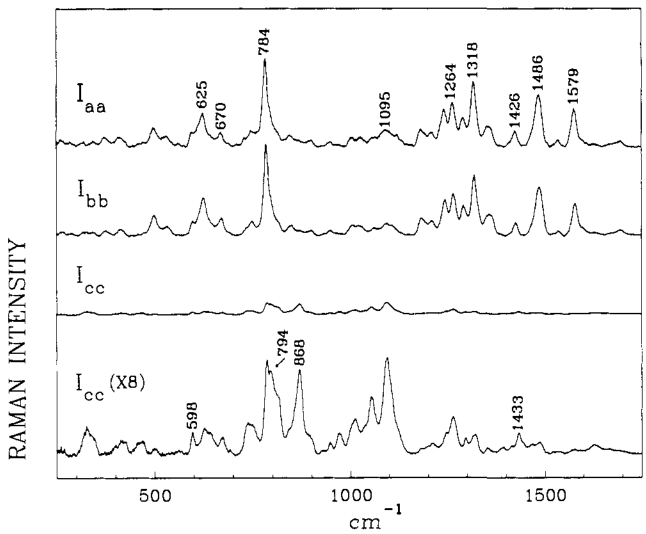

Figure 4. Raman spectra of the single crystal of d(CGCGCG), corresponding to three different orientations of the unit cell axes with respect to the electric vector of exciting and scattered radiation. From top-to-bottom: I_{aa}, crystallographic *a*-axis parallel to *X*; I_{bb}, crystallographic *b*-axis parallel to *X*; I_{cc}, crystallographic *c*-axis parallel to *X*; I_{cc} (×8), 8-fold amplification of the ordinate employed for I_{cc}. Spectra were collected with 514.5-nm excitation. Similar data (not shown) exhibiting identical band intensity ratios were obtained with 488.0-nm excitation.

(4) Using judiciously chosen trial values for r_1 and r_2, calculate I_{aa}/I_{bb}, I_{bb}/I_{cc}, and ρ from eqs 7, 8, and 9, respectively, and compare with the experimentally observed values. Tsuboi and co-workers[3,16,17] have presented a diagram showing parametric relationships among r_1, r_2, and ρ. This r/ρ diagram is useful for selecting judicious choices of r_1 and r_2 consistent with a given value of ρ.

(5) Revise the orientations of the principal axes and/or r_1 and r_2 and repeat the trial calculations of steps 2–4, above, until satisfactory agreement is reached between the calculated and observed values of I_{aa}/I_{bb}, I_{bb}/I_{cc}, and ρ.

Applications of the above procedure to local Raman tensors of aspartame[16] and mononucleotides[3,17] have been described. Extension to the Z-DNA crystal is described in the sections which follow.

Results and Discussion

1. Polarized Raman Spectra of the d(CGCGCG) Crystal. As indicated above, the *ab*, *bc*, and *ac* components of the Raman tensor are predicted to be very small for crystals of the $P2_12_12_1$ space group. This is the case for the d(CGCGCG) crystal. Virtually no Raman scattering intensity is detected when the polarizer is rotated from the *X* to the *Y* orientation of Figure 2. Thus, when the electric vectors of both the exciting and scattered radiation are along the *X* direction, the Raman intensities I_{aa}, I_{bb}, or I_{cc}, corresponding to *aa*, *bb*, or *cc* components of the crystal Raman tensor, are obtained by rotating the crystal in the X–Y plane until the appropriate crystallographic axis (*a*, *b*, or *c*, respectively) is coincident with *X* (Figure 2). We measured I_{aa}/I_{bb} with the *ab* face of the crystal oriented in the horizontal plane and I_{bb}/I_{cc} with the *bc* face oriented in the horizontal plane. We also recorded the Raman spectrum of the mother liquor at conditions identical to those employed for the crystal, in order to correct for the very small spectral contribution of the mother liquor. Representative spectral data obtained from the d(CGCGCG) crystal are shown in Figure 4.

As seen in Figure 4, the I_{aa} and I_{bb} spectra exhibit many similarities. However, there are a number of important differences, notably the 1579- and 1095-cm^{-1} bands are more intense in I_{aa} than in I_{bb}, whereas the 625- and 670-cm^{-1} bands are more intense in I_{bb} than in I_{aa}. The I_{cc} component of the spectrum is strikingly weaker than that in either I_{aa} or I_{bb}. An 8-fold expansion of the ordinate in the I_{cc} spectrum (Figure 4, bottom) clearly reveals the significantly different relative band intensities of I_{cc} in comparison to those of either I_{aa} or I_{bb}.

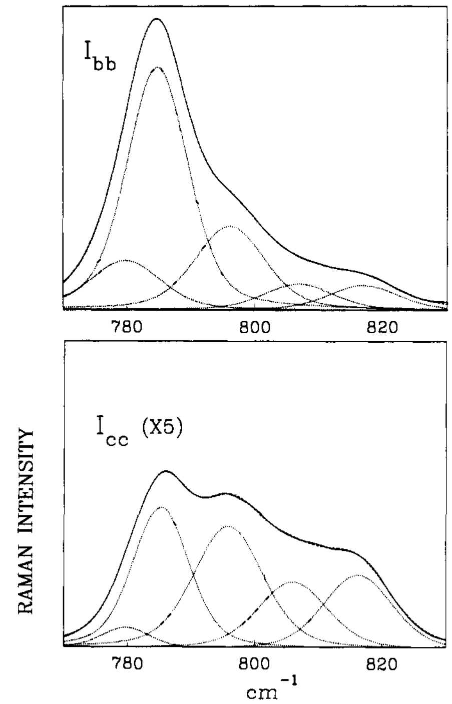

Figure 5. Decomposition of the complex Raman bandshape of the single crystal of d(CGCGCG) in the spectral region 760–830 cm^{-1} in terms of the minimum number (5) of Gauss-Lorentz components. Both I_{bb} (top spectrum) and I_{cc} (bottom spectrum, 5-fold expansion) are shown.

A complete set of Raman data like that shown in Figure 4 was also collected on the single crystal of d(CGCGCG) using 488.0-nm laser excitation. All band intensity ratios (I_{aa}/I_{bb}, and I_{bb}/I_{cc}) were the same as those observed with 514.5-nm excitation. In cases where significant overlap of Raman bands was encountered, intensity ratios were estimated by decomposition of the complex band shape into the minimum number of components required to accurately reproduce the band envelope. This is illustrated for the bands in the region 770–830 cm^{-1} in Figure 5. Experimentally determined Raman tensors for the d(CGCGCG) single crystal are given in Table III.

2. Depolarization Ratios of the Raman Bands and Implications for the Raman Tensors. The depolarization ratios of Raman bands of isotropic Z-DNA, as determined from poly(dG–dC)·poly(dG–dC) in 4 M NaCl solution, are listed in Table I. Included for comparison in Table I are depolarization ratios determined previously for aqueous solutions of the related mononucleotides 5′-GMP and 5′-CMP.[17] Interestingly, the ρ values of the guanine bands at 1318 and 1581 cm^{-1} (0.34 and 0.31, respectively) are essentially equal in poly(dG–dC)·poly(dG–dC) and 5′-GMP. This suggests that the shapes and orientations of the corresponding Raman tensors are nearly the same in the polynucleotide duplex and in the mononucleotide. Additionally, the depolarization ratios are independent of the choice of 514.5- or 488.0-nm excitation. The unexpectedly low depolarization ratio (ρ = 0.11) reported previously for the 1486-cm^{-1} band of the guanine ring of 5′-GMP[17] is confirmed also for poly(dG–dC)·poly(dG–dC) (ρ = 0.14). These findings together suggest that the normal mode in question is not related simply to the asymmetric ring stretching mode of similar frequency in benzene derivatives. Table I also shows that the symmetrical ring stretching vibration at 625 cm^{-1} (six-membered ring "breathing" mode) of guanine in poly(dG–dC)·poly(dG–dC) exhibits the expected very low value of ρ = 0.07, consistent with other ring breathing modes.

The ρ values for bands near 1427 cm^{-1} (CH_2 scissoring), 1266 cm^{-1} (asymmetric ring stretching in the cytosine residue), 1095

Table III. Experimental and Calculated Crystal Raman Tensors of d(CGCGCG)

band (cm^{-1})	residue	method[a]	I_{aa}/I_{bb}	I_{bb}/I_{cc}	ρ
1579	guanine	obs	1.2 ± 0.1	88 ± 3	0.33
		G1(-1, 23.4)	1.05	88	0.33
1486	guanine	obs	1.0 ± 0.1	43 ± 3	0.14
		G2(5, 9)	1.01	43	0.11
1426	$C2'H_2$	obs	1.0 ± 0.3	>20	0.4
		CH_2(-2, 10)	0.7	43	0.4
1433	$C5'H_2$	obs		<3	0.4
		CH_2(-2, 10)	1.3	1.8	0.4
1318	guanine	obs	1.0 ± 0.1	26 ± 3	0.31
		G3(-0.5, 10.8)	0.98	26	0.31
1264	cytosine	obs	1.0 ± 0.1	9.3 ± 0.5[b]	0.27
		C2(-0.2, 6.3)	0.98	9.3	0.27
1095	PO_2^-	obs	1.3 ± 0.2	1.1 ± 0.1	0.1
		P1(0.1, 0.5)	1.28	1.01	0.1
868	backbone	obs	1.0 ± 0.2	0.35 ± 0.02	<0.2
		D1(3.2, 1.8)	1.1	0.35	0.05
		P2(0.8, -0.16)	1.0	0.37	0.19
794	P-O	obs	1.0 ± 0.1	3.5 ± 0.2	
		P2(1, 6)	1.1	3.5	0.2
784	cytosine	obs	1.0 ± 0.1	8.8 ± 0.3	0.06
		C1(2.5, 3.7)	1.0	8.7	0.06
745	P-O	obs	1.0 ± 0.1	3.2 ± 0.3	<0.3
		P2(2.5, 10)	1.0	3.1	0.18
670	guanine	obs	0.93 ± 0.03	8.0 ± 0.5	0.07
		G3(2.75, 2.95)	0.93	8.0	0.04
625	guanine	obs	0.94 ± 0.03	11.6 ± 0.5	0.07
		G3(3.85, 3.25)	0.94	11.3	0.06
598	cytosine	obs	1.1 ± 0.1	4.3 ± 0.5	0.17
		C1(0.5, 3.8)	1.00	4.3	0.16

[a] The experimentally observed (obs) or representative calculated tensor quantity (notation of Table II) is indicated. For the calculated tensor, the assumed pair of parameters (r_1, r_2) is given in parentheses. [b] Estimate based upon the measured peak height at 1264 cm^{-1}, uncorrected for possible overlap of neighboring bands.

cm^{-1} (PO_2^- symmetric stretching), and 596 cm^{-1} (in-plane ring deformation of the cytosine residue) are all nearly equal for poly(dG–dC)·poly(dG–dC) and nucleotide model compounds. Therefore, these vibrations and changes in the shapes and orientations of their respective Raman tensors may be considered largely localized in the designated groups of atoms.

In poly(dG–dC)·poly(dG–dC), the broad band near 785 cm^{-1} exhibits ρ = 0.12, larger than expected for the cytosine ring breathing mode near this frequency (cf. 5'-CMP, Table I, for which the 785-cm^{-1} band exhibits ρ = 0.064). This is attributed to overlap of the cytosine band of poly(dG–dC)·poly(dG–dC) with the less strongly polarized band near 796 cm^{-1} due to a localized DNA backbone vibration.[8,21,22] Accordingly, we employ ρ = 0.064 as the appropriate depolarization ratio for the band due to the ring breathing mode of cytosine.

The depolarization ratios which facilitate calculation of the Raman tensors of d(CGCGCG) in accordance with the procedural algorithm outlined in section 3 of Materials and Methods are given in the last three columns of Table I.

3. Analysis and Interpretation of the Polarized Raman Spectra. As seen in Figure 4, Raman bands of the I_{cc} spectrum at 1579, 1486, 1318, 1264, 784, 670, and 625 cm^{-1} are much weaker than their counterparts in the I_{aa} and I_{bb} spectra. This observation is consistent with the crystal structure,[2] in which all base planes are arranged nearly in the *ab* plane, i.e. nearly perpendicular to the *c*-axis. Thus, for the Raman tensor corresponding to each band, at least one in-plane component (α_{xx} or α_{yy}) must be much greater than the out-of-plane component (α_{zz}). Additionally, for the 1579-, 1318-, and 1264-cm^{-1} bands, α_{xx} and α_{yy} are expected to differ significantly from one another,[17] and in principle, such a

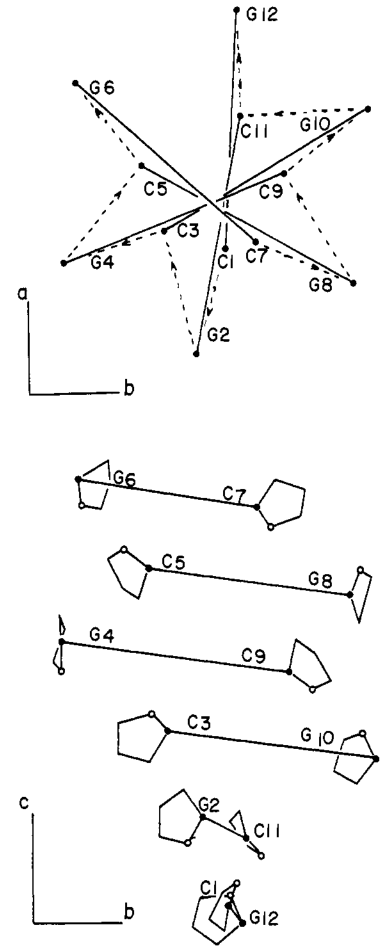

Figure 6. Diagrams of the d(CGCGCG) crystal structure based upon X-ray coordinates of Gessner et al.[2] as viewed along the *c*-axis (top) and *a*-axis (bottom). Each base pair is represented by a straight line connecting the glycosyl C1' atoms (filled circles). The O4' atoms (open circles) of the deoxyribose rings are also shown.

difference should be reflected in the intensity ratio, I_{aa}/I_{bb}. However, in the d(CGCGCG) crystal, the arrangement of bases in the *ab* plane is pseudo-6-fold symmetric as illustrated in Figure 6. Thus, the potentially informative I_{aa}/I_{bb} ratio is lost in the measurements on the hexanucleotide duplex, and relative magnitudes of the α_{xx} and α_{yy} components for these vibrations cannot be determined directly.

The weak band at 1426 cm^{-1} in I_{aa} and I_{bb} spectra, assigned to CH_2 scissoring, is not evident in the I_{cc} spectrum, where instead a weak band is observed at 1433 cm^{-1}. This is explained by the existence of two distinct CH_2 scissoring bands, assignable to $C2'H_2$ and $C5'H_2$ groups, respectively. The crystal structure reveals that most $C2'H_2$ groups are oriented such that a line connecting the hydrogens is approximately perpendicular to the *c*-axis.[2] Since the H···H axis is the direction along which the Raman tensor should have its greatest component,[17] the corresponding Raman band should exhibit much greater intensity in the I_{aa} and I_{bb} spectra than in the I_{cc} spectrum. On this basis, the 1426-cm^{-1} band may be reasonably assigned to the $C2'H_2$ groups, and the 1433-cm^{-1} band, to the $C5'H_2$ groups.

The 1095-cm^{-1} band, assignable to the symmetric stretching vibration of the anionic phosphodioxy group $(O–P–O)^-$, gives similar intensities in all polarized spectra. This is as expected, because the 10 PO_2^- groups per asymmetric unit are oriented along markedly different directions.[2] Additionally, the Raman tensor of this vibration is expected to be intrinsically rather isotropic.

The Raman band at 868 cm^{-1} draws special attention. This is the only band that is demonstrably more intense in the I_{cc}

(21) Benevides, J. M.; Thomas, G. J., Jr. *Nucleic Acids Res.* **1983**, *11*, 5747–5761.
(22) Prescott, B.; Steinmetz, W.; Thomas, G. J., Jr. *Biopolymers* **1984**, *23*, 235–256.

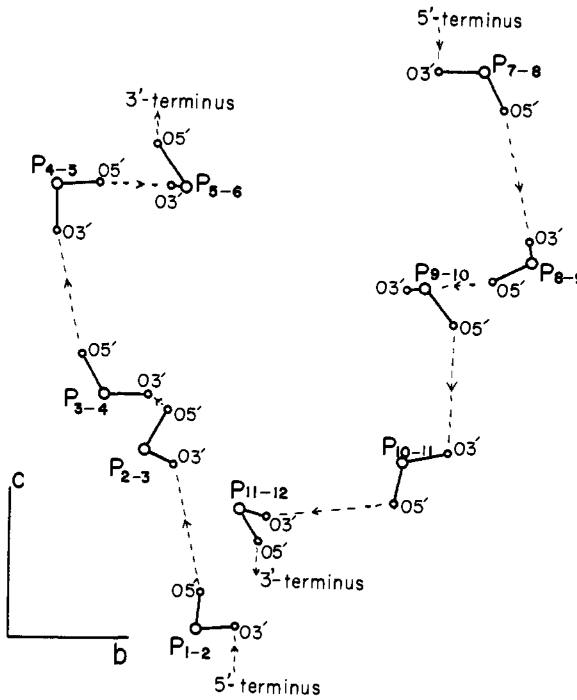

Figure 7. Diagram of the d(CGCGCG) crystal structure based upon X-ray coordinates of Gessner et al.[2] illustrating the orientations of ester P–O5′ and P–O3′ bonds in the asymmetric unit. The view is along the *a*-axis.

spectrum than in either the I_{aa} or I_{bb} spectrum. The Raman tensor of the 868-cm^{-1} band, therefore, exhibits its greatest component along the crystallographic *c*-axis. On the basis of the crystal structure[2] and model compound studies[3,17] (Y. Guan and G. J. Thomas, Jr., unpublished results), two types of vibrational modes localized in the deoxyribose–phosphate moiety may be considered as reasonable candidates for the 868-cm^{-1} band assignment. These are P–O5′ stretching and furanose ring breathing. As seen in Figure 7, many of the P–O5′ bonds of the asymmetric unit are directed nearly along the *c*-axis, which could account for the observed polarization characteristics. Alternatively, Figure 6, shows that all furanose rings are arranged with their "planes" parallel to the *c*-axis and with the ∠C1′–O–C4′ angle bisectors nearly parallel to the *c*-axis. It is possible that one component of the Raman tensor is localized along the bisector, and that this Raman tensor component is much greater than the other two, thus accounting for the observed anisotropy. We tentatively assign the 868-cm^{-1} band to the deoxyribose–phosphate moiety; however, further elucidation of the specific character of the vibration will require additional polarized Raman studies of isotopically modified DNA structures.

4. Raman Scattering Tensors. (a) Guanine. For the 1579-cm^{-1} band of guanine, we find that $I_{bb}/I_{cc} = 88$. This extraordinarily high value, together with the moderately high value observed for the depolarization ratio ($\rho = 0.33$), indicates that either r_1 or r_2, but not both, is large.[17] By use of the r/ρ diagram, we find that the values $r_1 = -1$ and $r_2 = 23$ are most consistent with the data. In other words, when the normal coordinate of this vibration increases, the molecular polarizability increases greatly along one in-plane axis, whereas the polarizability slightly decreases along the other in-plane axis and slightly increases in the out-of-plane direction. For the 1318-cm^{-1} band of guanine, the anisotropy ($r_1 = -0.5$ and $r_2 = 10.8$) is similar to, but not as extreme as, that of the 1579-cm^{-1} band.

As noted previously, the pseudo-6-fold symmetry of the hexamer duplex prevents a unique determination of the in-plane Raman tensor axes for base residues related by a screw axis of symmetry. Thus, although the in-plane axis of large polarizability change is not determined uniquely by the data, it is possible to select arbitrary configurations of the principal axes which are consistent with the data. Three of these are shown in Figure 4 (top), and the corresponding calculations of localized Raman tensors for both the 1579- and 1318-cm^{-1} bands are given in Table IV.

Table IV. Raman Tensors of Localized Vibrations of the Guanine Residue

band (cm^{-1})	experimental results I_{aa}/I_{bb}	I_{bb}/I_{cc}	ρ	method[a]	calculated results I_{aa}/I_{bb}	I_{bb}/I_{cc}	ρ
1579	1.2 ± 0.1	88 ± 3	0.33	G1(−1, 23.4)	1.05	88.1	0.33
				G2(−1, 21.6)	1.02	87.1	0.33
				G3(−1, 20.6)	0.98	88.7	0.33
1486	1.0 ± 0.1	43 ± 3	0.14	G1(4.3, 10)	1.03	43.0	0.13
				G2(5, 9)	1.01	43.3	0.11
				G3(5, 9.5)	1.01	43.2	0.11
1318	1.0 ± 0.1	26 ± 3	0.31	G1(−0.5, 12)	1.05	27.1	0.31
				G2(−0.5, 11.2)	1.02	25.8	0.31
				G3(−0.5, 10.8)	0.98	26.0	0.31
670	0.93 ± 0.03	8.0 ± 0.5	0.07	G1(3, 2.8)	0.93	8.2	0.04
				G2(2.5, 3.25)	0.93	8.1	0.05
				G3(2.75, 2.95)	0.93	8.0	0.04
625	0.94 ± 0.03	11.6 ± 0.5	0.07	G1(3.1, 3.6)	0.93	11.1	0.05
				G2(4, 2.7)	0.94	11.0	0.06
				G3(3.85, 3.25)	0.94	11.3	0.06

[a] Nomenclature as defined in Figure 3 and Table III.

As seen here, a typical set of r_1 and r_2 values is nearly independent of the choice of axis system. Examination of the first three rows of Table IV indicates, however, that in order to obtain a satisfactory fit to the experimental data it is necessary to choose smaller values of r_2 on going from coordinate system G1 ($r_2 = 23.4$) to G2 (21.6) to G3 (20.6), if r_1 is maintained constant at −1. This is also the case for the 1318-cm^{-1} band, as shown in rows 7–9 of Table IV. These relationships reflect the fact[2] that the guanine base planes are not exactly perpendicular to the crystallographic *c*-axis but are slightly tilted, and that the tilting for all six guanine residues is nearly along the *y*-axis of the G3 coordinate system (Figure 3).

The 1486-cm^{-1} band of guanine, like the corresponding band in adenine,[17] exhibits also an unexpectedly small depolarization ratio ($\rho \approx 0.1$). Other base vibrations of the 1200–1600-cm^{-1} region ordinarily exhibit much greater ρ values. The ρ and I_{bb}/I_{cc} data indicate ranges of $4 < r_1 < 5$ and $9 < r_2 < 10$. Therefore, for the 1486-cm^{-1} vibration, it is established that the polarizability change is much greater in any pair of orthogonal in-plane directions than in the out-of-plane direction, and further that α_{xx}, α_{yy}, and α_{zz} have the same sign. Again however, orientations of the *x* and *y* axes within the base plane are not uniquely determined, as is evident from Table IV.

We include in Table IV the results obtained for the guanine "ring-breathing" bands at 670 and 625 cm^{-1}. The 670- and 625-cm^{-1} bands in the d(CGCGCG) crystal are the two well-known deoxyguanosine conformation markers (C3′-endo/syn and C2′-endo/syn, respectively).[12] Present calculations of I_{aa}/I_{bb} and I_{bb}/I_{cc} (eqs 7 and 8) were made on the basis of the previous assignment that the 670-cm^{-1} band is due to the two terminal dG residues (C2′-endo/syn) and the 625-cm^{-1} band to the four internal dG residues (C3′-endo/syn).[12] As expected from the ρ values observed for these vibrations (Table I), anisotropy of the Raman tensors is much less than occurs for other guanine ring modes (Table IV). Specifically, α_{zz} is determined to be about one-third as large as α_{xx} and α_{yy}, leading to a more spherically shaped Raman tensor.

(b) Cytosine. The 1264-cm^{-1} band of cytosine, like most base residue vibrations of the 1200–1600-cm^{-1} interval, is expected to have an anisotropic Raman tensor. With $I_{bb}/I_{cc} = 9.3$ and $\rho = 0.29$, we find that either $r_1 << r_2$, or the converse, would fit the experimental data. Good agreement is obtained for $r_1 = -0.2$ and $r_2 = 6.3$, or alternatively, for $r_1 = 6.9$ and $r_2 = 0.13$ (Table

Table V. Raman Tensors of a Localized Vibration of the Cytosine Residue

band (cm^{-1})	experimental results			method[a]	calculated results		
	I_{aa}/I_{bb}	I_{bb}/I_{cc}	ρ		I_{aa}/I_{bb}	I_{bb}/I_{cc}	ρ
1264	1.0 ± 0.1	9.3 ± 0.5	0.27[b]	C1(−0.2, 6.8)	1.01	9.36	0.28
				C2(−0.2, 6.3)	0.98	9.28	0.27
				C3(−0.2, 6.1)	0.96	9.34	0.27
				C1(6.9, 0.13)	1.01	11.6	0.25
				C2(6.9, 0.13)	1.02	9.90	0.25
				C3(6.9, 0.13)	1.06	9.26	0.25

[a] Nomenclature as defined in Figure 3 and Table III. [b] Average of experimental values for poly(dG–dC)·poly(dG–dC) and 5′-CMP (Table I).

V). Although the pseudo-6-fold symmetry of the crystal (Figure 6, top) again prevents complete determination of the tensor shape in question, the results of trial calculations shown in Table V suggest a few important characteristics of the tensor. First, each of the three choices of cytosine principal axes (C1, C2, or C3 of Figure 3) leads to the conclusion that one of the in-plane tensor components (α_{xx} or α_{yy}) must be 6–7 times greater than the out-of-plane component (α_{zz}), and the other in-plane component must be very small. This conclusion is independent of the choice of axes. Second, among the three representative coordinate systems of Figure 3, C3 requires the smallest α_{yy} (smallest r_2) in order to fit the experimental data satisfactorily (Table V). This allows us to infer that the direction of y in the system C3 is nearly parallel to the axis of slight tilt which is revealed in the X-ray crystal structure.[2] Third, this slight tilting should in principle be useful in evaluating the relative merits of the C1, C2, and C3 axis systems. For example, if future experimental data permit fixing $r_1 = 6.9$ and $r_2 = 0.13$ (Table V), then C3 would be established as superior to C2 or C1.

The 784-cm^{-1} band is assigned to the ring breathing vibration of the cytosine residue. On the basis of its lower depolarization ratio ($\rho = 0.064$), the Raman tensor for this mode must be less anisotropic than that of the 1264-cm^{-1} band. However, because I_{bb}/I_{cc} is as high as 9.5, α_{zz} must be appreciably smaller than α_{xx} and α_{yy}. With principal axis system C1 (Figure 3), we find that $r_1 = 2.5$ and $r_2 = 4$.

The 598-cm^{-1} band of cytosine has a rather high value of ρ (0.17), and therefore a fairly anisotropic Raman tensor. Since $I_{bb}/I_{cc} = 4.3$, we obtain $r_1 = 0.5$ and $r_2 = 3.8$ with the C1 principal axes. This indicates that the normal coordinate for the 598-cm^{-1} vibration involves an in-plane ring deformation of the cytosine residue, and implies a large polarizability change along only one in-plane direction.

(c) Backbone. As noted previously,[17] the Raman bands ca. 1420–1430 cm^{-1} due to CH_2 scissoring modes give $\rho \approx 0.4$, indicative of a highly anisotropic Raman tensor. In general, therefore, the orientation of a CH_2 group in an oriented sample may be determined from its polarized Raman spectrum. In d(CGCGCG), we find two distinct CH_2 bands, at 1426 and 1433 cm^{-1}, assigned respectively on the basis of their polarization characteristics to the C2′H_2 and C5′H_2 groups. More detailed examination of the data indicates $I_{bb}/I_{cc} \geq 20$ for the 1426-cm^{-1} band, and $0 < I_{bb}/I_{cc} < 3$ for the 1433-cm^{-1} band. It is interesting to note (Table III) that the same set of r_1 (=−2) and r_2 (=10) values explains both of the observed I_{bb}/I_{cc} spectra. This provides strong support for the vibrational assignments. We note also that the 1433-cm^{-1} band is relatively weak in comparison to the 1426-cm^{-1} band, despite equal numbers of C2′H_2 and C5′H_2 groups in the asymmetric unit. This may be attributed to the relatively random orientation of C5′H_2 groups in comparison to C2′H_2 groups. The latter are oriented with their principal axis of greatest polarizability change (y) nearly perpendicular to the c-axis. Thus, it is not surprising that the 1426-cm^{-1} band exhibits higher intensity in the I_{aa} and I_{bb} spectra.

Our present analysis of the 1095-cm^{-1} band shows that both r_1 and r_2 are less than 1 for the P1 axis system (Figure 4 and Table III). This indicates that the PO_2^- symmetric stretching vibration causes a greater polarizability change along the direction perpendicular to the OPO plane than along the in-plane directions. This interpretation is based upon the fact that I_{aa}/I_{bb} and I_{bb}/I_{cc} are both >1. This set of r_1 and r_2 values, however, should be regarded as an average for the 10 inequivalent PO_2^- groups. As seen in the I_{aa} spectrum of Figure 4, the band observed near 1095 cm^{-1} is extraordinarily broad and appears to mask a fine structure consisting of a few overlapping components. This is also the case for the I_{bb} spectrum, although the band shape here is different from that of the I_{aa} spectrum. On the other hand, the band near 1095 cm^{-1} in the I_{cc} spectrum is relatively sharp and presumably less complex. These observations suggest that not all of the 10 PO_2^- groups per hexamer duplex have identical I_{aa}/I_{bb} and I_{bb}/I_{cc} values. This is not surprising, since the PO_2^- groups are located in different crystal environments. In addition, the crystal structure shows that some of the intramolecular P···P distances are less than 7 Å,[2] for which transition dipole coupling between PO_2^- symmetric stretching vibrations may be appreciable.[23] It should also be pointed out that the x-axis of the tensor may deviate appreciably from the bisector of the ∠OPO angle, as defined in the P1 system. To further refine the Raman tensor of the PO_2^- symmetric stretching vibration, data from other oligonucleotide crystals are required.

It is important to elucidate the nature of the normal modes generating Raman bands of the DNA backbone in the 700–900-cm^{-1} interval. In the d(CGCGCG) crystal, we find three prominent Raman bands in this interval, at 868, 796, and 745 cm^{-1}. The respective I_{bb}/I_{cc} values are 0.35, 3.5, and 3.2. If one of these were a pure O–P–O symmetric stretching vibration, like the 757-cm^{-1} band of $(CH_3O)_2PO_2^-$ (Y. Guan and G. J. Thomas, Jr., unpublished results), then the P1 coordinate system should apply. However, none of the I_{bb}/I_{cc} values can be reproduced using P1 and eq 8 with plausible limits for r_1 and r_2. Hence, we find that none of the 868-, 796-, and 745-cm^{-1} bands can be reasonably assigned to a pure O–P–O symmetric stretching mode. We adopted P2 as a second trial coordinate system. Calculations with this system indicate that r_1 should be small ($1 < r_1 < 2.5$) and r_2 should be large ($7 < r_2 < 10$) for both the 796- and 745-cm^{-1} bands. Thus, another important finding is that the normal modes at 796 and 745 cm^{-1} both involve large polarizability changes along the P–O3′ bond.

5. Comparison with Previous Work. Patapoff et al.[24] measured the polarized Raman spectrum of a single crystal of d-(AAAAATTTTT), which exhibits Raman markers of the B form, although no X-ray crystal structure of d(A_5T_5) has been published. The Raman spectrum of the d(A_5T_5) crystal (Figure 6 of ref 24) is dramatically different from that of the d(CGCGCG) crystal (spectrum I_{aa} in Figure 4, above), as expected from the dissimilar secondary structures and different base compositions of these oligomers. Nevertheless, the Raman measurements of d(A_5T_5) for orthogonal orientations of the long axis of the crystal with respect to the laser polarization direction[24] bear certain similarities to the anisotropies we have measured for d(CGCGCG). Specifically, Patapoff et al. found α_{zz} of d(A_5T_5) very weak, and $\alpha_{xy} \approx \alpha_{xz} \approx 0$. We find α_{cc} of d(CGCGCG) very weak, and $\alpha_{ab} \approx \alpha_{ac} \approx 0$. Further, both d($A_5T_5$) and d(CGCGCG) crystals exhibit intensities for their symmetric PO_2^- stretching modes (bands ca. 1100 cm^{-1}) which are not strongly dependent upon the orientation of the crystal with respect to the laser polarization direction.

It should be emphasized, however, that our approach is fundamentally different from that of Patapoff et al.[24] We have

(23) Tsuboi, M.; Nishimura, Y. *Raman Spectroscopy, Linear and Nonlinear*; Lascombe, J., Huang, P. V., Eds.; Wiley: New York, 1982; pp 683–693.
(24) Patapoff, T. W.; Thomas, G. A.; Wang, Y.; Peticolas, W. L. *Biopolymers* **1988**, *27*, 493–507.

made use of the known X-ray crystal structure of d(CGCGCG) to determine the crystal Raman tensors, and we have combined the results with measured depolarization ratios to estimate Raman scattering tensors applicable to the normal modes of the DNA nucleotide residues. Conversely, the X-ray crystal and molecular structures of $d(A_5T_5)$ are not known. The present study provides the first step toward elucidating local Raman tensors of DNA, which may serve eventually to facilitate a better quantitative understanding of oligonucleotide crystals of unknown three-dimensional structure, such as $d(A_5T_5)$. In fact, the present results allow the inference that the base planes of the $d(A_5T_5)$ crystal are likely perpendicular to the long axis of the single crystal.[24]

Finally, the importance of the present approach is underscored by the fact that the out-of-plane component (α_{zz}) of a Raman tensor associated with an in-plane vibration of an aromatic ring is not always small. For example, α_{zz} for the 992-cm^{-1} vibration of benzene is 61% of α_{xx}.[17]

Summary and Conclusions

Polarized Raman microscopy of the Z-DNA single crystal, d(CGCGCG), reveals the large anisotropies expected for the crystallographic $P2_12_12_1$ space group. For the crystal Raman tensor components, we find $I_{ab} \approx I_{bc} \approx I_{ac} \approx 0$, $I_{aa} \neq 0$, $I_{bb} \neq 0$, and $I_{cc} \neq 0$. The results indicate that the DNA duplex of the asymmetric unit is arranged with the helical axis oriented along the crystallographic *c*-axis, in accordance with the X-ray crystal structure.

The instrumentation (Figure 2) and experimental procedures demonstrated here allow accurate, reproducible, and nondestructive measurement of the crystal Raman tensors without removal of the crystal from the thermostated mother liquor environment. Use of the confocal microscope probe reduces Raman interference from the mother liquor to virtually negligible levels. Although small mother liquor corrections were implemented in the present data analyses, neglect of the mother liquor contributions leaves the results essentially unchanged.

The major conclusions of this work are the following. (i) The crystal Raman tensors of double-helical DNA are determined reliably by confocal Raman microscopy of the DNA single crystal. (ii) Use of a simple theoretical model allows the crystal Raman tensors to be related directly to the localized molecular Raman tensors. (iii) For each vibrational mode of d(CGCGCG) yielding a Raman band of at least moderate intensity, the relative polarizability changes along the principal axes have been deduced.

We have used the anisotropies measured from polarized Raman spectra to propose several specific and new Raman band assignments for Z-DNA. Thus, the bands at 1426 and 1433 cm^{-1} have been assigned, respectively, to CH_2 scissoring vibrations of the 2′ and 5′ carbons of the Z-DNA backbone. Additionally, the 868-cm^{-1} band of Z-DNA has been identified as due to a vibrational mode of the deoxyribose–phosphate backbone. The absence of a Raman band of similar frequency in the DNA A form, or of comparable intensity in the B form, demonstrates the conformational sensitivity of this mode. By analysis of the polarized Raman data and residue bond orientations in the d(CGCGCG) crystal structure, we have determined further that the 868-cm^{-1} band may be assigned to the deoxyribose–phosphate moiety, and more specifically to either furanose ring breathing or P–O5′ bond stretching or a combination of such motions. Conversely, we have concluded that the Raman bands at 796 and 745 cm^{-1} involve large participations of P–O3′ bond stretching.

The present study provides a first step in the determination of localized molecular Raman tensors of DNA. Extension of this analysis to other DNA single crystals and fibers, including AT-containing sequences, is in progress. The combined results will permit the determination of residue orientations in DNA of unknown conformation. Thus, with the data base being developed here, it should be possible to interpret Raman anisotropies measured on altered states of DNA and its complexes in terms of specific geometric configurations of the nucleotide residues. Examples include the determination of base, sugar, and phosphate orientations in packaged ssDNA of filamentous viruses, orientations of dsDNA packaged in icosahedral viral capsids, and residue configurations in multistranded DNA complexes (e.g. H-DNA and telomeric DNA).

Acknowledgment. Support of this research by Grant AI18758 from the U.S. National Institutes of Health and Grant No. 02670985 from the Ministry of Education, Science and Culture (Japan) is gratefully acknowledged.